Fuzzy and Extra Crisp Alternating Projection onto Convex Sets (POCS)

Robert J. Marks II, Loren Laybourn & Shinhak Lee
Department of Electrical Engr., University of Washington, Seattle, WA 98195

Seho Oh
Neopath, 1750 112th Avenue NE, Bellevue, WA 98004

Abstract— *Alternating projections onto convex sets* (POCS) is a powerful tool for signal and image restoration and synthesis. Convex sets of signals obeying desired constraints are first specified. Then, by repeated projection onto these sets, convergence is to a signal obeying all desired constraints. The method assumes, however, that there is a nonempty intersection of the sets. If the intersection is empty, the result of POCS is not unique and, if the sets are not 'close', generally considered to be of little use. To construct sets that are closer, one or more of the convex sets is fuzzified. The α-cuts of the fuzzified sets, also convex, will eventually result in constraints with a nonempty intersection. Using a fuzzification of the convex constraint set allows approximate satisfaction of inconsistent constraints. Example applications are presented for computer tomography and optical diffraction synthesis.

I. Introduction

Alternating projections onto convex sets (POCS) [1, 2] is a powerful technique of signal recovery and synthesis. A (crisp) set, C, is convex if $g_1 \in C$ and $g_2 \in C$ implies that $\lambda g_1 + (1-\lambda)g_2 \in C$ for all $0 \leq \lambda \leq 1$.

The projection onto a convex set is geometrically illustrated in Figure 1. For a given $g \notin C$, the projection onto C is the unique vector $f \in C$ such that the mean square distance between f and g is minimum[1] . If $g \in C$, then the projection onto C is g.

Given two or more convex sets with nonempty intersection, alternately projecting among the sets will converge to a point included in the intersection [2]. This is geometrically illustrated in Figure 2. If two convex sets do not intersect, then convergence is to a limit cycle that is a mean square solution to the problem. Specifically, the cycle is between points in each set that are closest in the mean square sense to the other set [3]. This is illustrated in Figure 3.

[1]The space is assumed throughout to be either L_2 or ℓ_2. The mean square distance is the corresponding norm.

0-7803-2461-7/95/$4.00 © 1995 IEEE

POCS was apparently first reported by Bregman [5] and Gubin *et al.* [6]. For the specific case of intersecting linear varieties (hyperplanes), POCS is, as a special case, Von Neumann's alternating projection theorem [4, 7, 8]. POCS was popularized by Youla [2] and Stark [1, 9].

Fuzzy POCS

Fuzzy convex sets were introduced in Zadeh's seminal paper [12, 13, 15, 16]. Let the fuzzy set C_f have a membership function $\mu_{C_f}(\cdot)$. Let C_f^α denote an α-cut of C_f. The fuzzy set C_f is convex if all of its α-cuts ($0 \leq \alpha \leq 1$) are convex.

POCS breaks down in the important case where three or more convex sets do not intersect [10]. POCS, rather, converges to greedy limit cycles that are dependent on the ordering of the projections and do not display any desirable properties. This is geometrically illustrated in Figure 4. We propose, however, that optimization using fuzzy constraints [11, 18] can be applied to find valuable POCS solutions that are, in some sense, close [13] to each of the convex constraints. The underlying concept of 'close' suggests a fuzzification of the nonintersecting convex sets to fuzzy convex sets [14]. Even if three or more crisp sets do not intersect, α-cuts of their fuzzification can. This is illustrated in Figure 5. Even if fuzzy POCS does not result in a fixed point solution, the extent of the limit cycle is reduced.

Those seeking a more detailed introduction to fuzzy POCS are referred to Oh and Marks [17]. They show specific application of fuzzy POCS to the solution of a set of ill-conditioned linear equations and to signal extrapolation.

We will give a brief review of fuzzy POCS followed by example applications in diffraction synthesis and tomography.

Fuzzified Convex Sets and Their Projections

Two methods of fuzzification of crisp convex sets of signals to fuzzy convex sets are useful in fuzzy POCS. If the crisp

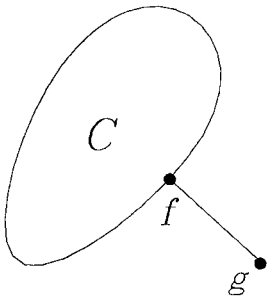

Figure 1: The point f is the projection of point g onto the convex set C.

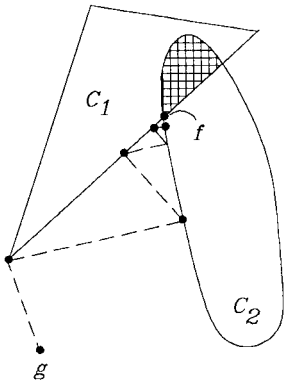

Figure 2: Alternately projecting between two or more convex sets with a nonempty intersections results in a limit point common to all sets (shown shaded here). Initiation at g converges to the point f on the intersection of convex sets C_1 and C_2.

convex set is parameterized, the fuzzy convex set, in many cases, can be generated by fuzzification of the parameter set. If the parameter set exists on an interval (*e.g.* $0 \leq$ Bandwidth $\leq \Omega$ for a set of bandlimited functions and $0 \leq$ Energy $\leq E_0$ for a set of signals with energy less than or equal to E_0) then the signal set is trivially convex. Fuzzification can be achieved simply by fuzzification of the interval [11]. This is illustrated in Figure 6. Equivalently, fuzzification can be achieved by dilation [17, 19, 29] of the underlying crisp set with a convex dilation kernel. If the dilation kernel is convex, then the dilation result can be interpreted is an α-cut of a fuzzy convex set [17]. The degree of membership of a signal in the fuzzy signal set is equal to that of the membership of the parameter in the fuzzified parameter set. This is illustrated in Figure 6.

If the crisp set of functions is not parameterized, fuzzification can be achieved through the direct morphological dilation [29] of each signal in the set. By choosing convex dilation kernels of increasing dimension, α-cuts of the fuzzified convex set can be generated [17].

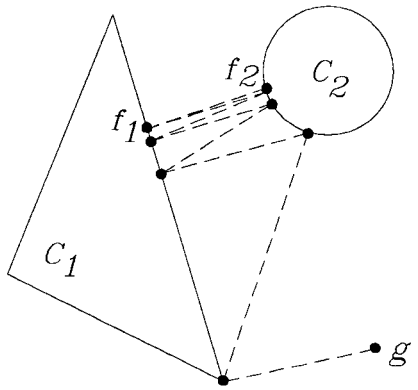

Figure 3: Projection between two non-intersecting convex sets results in a minimum mean square limit cycle. Point f_1 is the point in C_1 closest to C_2.

Fuzzy POCS of another sort can be applied to the case where two or more convex sets intersect in more than one point. The intersection of two or more convex sets is convex. By application of morphological erosion [29] to one or more component sets, convergence to interior points of the intersection, if they exist, can be obtained. In Figure 2, for example, convergence would be to a point within rather than on the shaded area. The approach is similar to the peeling away of convex hulls to find the most interior of a set of points [21]. This operation will not be considered here.

II. Diffraction Synthesis (Beam Forming and Holography)

POCS type synthesis of computer generated algorithms has been applied to cases where an image is desired at a single distance from an aperture [22]. For the single image synthesis problem, the convex sets of the underlying problem intersect. When the problem is generalized to two or more images, the sets do not intersect. Application of conventional POCS can result in a significant variation in image quality. Fuzzy POCS can be used to tune uniformity in the image quality.

To illustrate, consider the diffraction system shown in Figure 7. An aperture with transmittance $f(x, y)$ is illuminated from the right by planar monochromatic coherent illumination with wavelength λ. The beam will propagate a distance of z_1. On this plane, we require the diffracted beam to satisfy some constraint corresponding to a set of planar field amplitudes, $\mathcal{C}_1$. The beam propagates an ad-

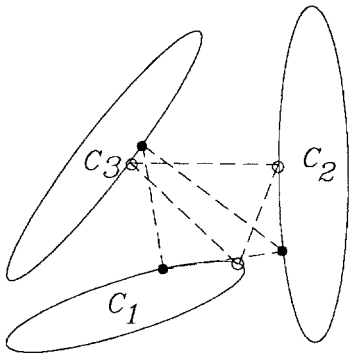

Figure 4: Projection between three or more nonintersecting convex sets results in greedy limit cycles. The path with solid points corresponds to a projection or der of 123. The path with hollow points corresponds to the path 132.

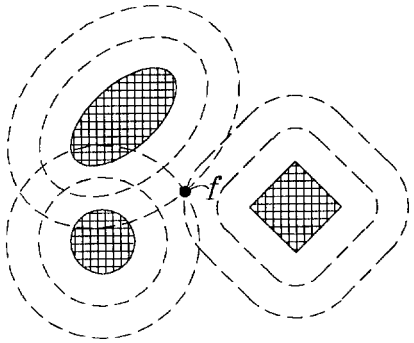

Figure 5: Three nonintersecting convex sets, shown shaded, are fuzzified through morphological dilation. Shown are contours of two alpha cuts. The three convex sets corresponding to the larger of the contours intersect in at the pont f which is 'close' to each of the three constraint sets.

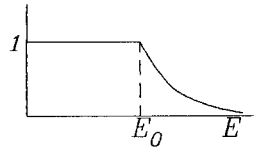

Figure 6: Fuzzification of the constraint set of signals with energy less than E_0.

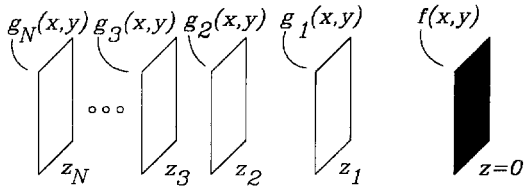

Figure 7: The diffraction synthesis problem is to construct a transmittance, $f(x,y$, so that the diffracted beam at various distances, z, obey given constraints.

ditional distance to z_2 where a constraint set $\mathcal{C}_2$ must be satisfied, etc. A total of N planes corresponds to N constraints. For the nth plane, we define the pupil function

$$p_n(x,y) = \begin{cases} 1 & ;\text{in the pupil} \\ 0 & ;\text{outside} \end{cases} \quad (1)$$

The constraint on the nth plane is that the field amplitude must be equal to zero outside of the nth pupil.

The diffraction in Figure 7 is governed by the Helmholtz equation [28]. All electric fields that satisfy the Helmholtz equation form a convex set[2]. For an aperture transmittance of $f(x,y)$, the electric field amplitude on the nth plane, $g_n(x,y)$, can be computed using the propagation of the angular spectrum [28].

$$\begin{aligned} g_n(x,y) &= \int_{-\infty}^{\infty}\int_{-\infty}^{\infty} F(u,v) \\ &\times \exp\left(-jk\sqrt{1-(\lambda u)^2-(\lambda v)^2}\right) \\ &\times e^{j2\pi(ux+vy)}du\,dv \end{aligned} \quad (2)$$

where

$$k = \frac{2\pi}{\lambda}$$

and $F(u,v)$ is the Fourier transform of $f(x,y)$,

$$F(u,v) = \int\int_{\text{aperture}} f(x,y)e^{-j2\pi(ux+vy)}dx\,dy \quad (3)$$

The angular spectrum solution in Equation 3 satisfies the Helmholtz equation.

To project the aperture, $f(x,y)$, onto the nth constraint set, the field $g_n(x,y)$ is first computed using Equation 2. This field is multiplied by the nth pupil to form

$$q_n(x,y) = p_n(x,y)g_n(x,y) \quad (4)$$

and back projected to the aperture plane to form

[2]A subspace

$$f_n(x,y) = \int_{-\infty}^{\infty}\int_{-\infty}^{\infty} Q_n(u,v) \times \exp\left(jk\sqrt{1-(\lambda u)^2-(\lambda v)^2}\right) \times e^{j2\pi(ux+vy)}du\,dv \quad (5)$$

where $Q_n(u,v)$ is the Fourier transform of $q_n(x,y)$. The function $f_n(x,y)$ is the projection onto the constraint set imposed by the nth plane. To avoid the degenerate solution $f(x,y) \equiv 0$, we will also require that

$$\int_{-\infty}^{\infty}\int_{-\infty}^{\infty} \Re\, q_n(x,y)\,dx\,dy = c \quad (6)$$

where $\Re$ denotes 'the real part of' and c is a constant. The set of all functions satisfying Equation 6 is convex[3]. If the pupils are of finite extent and $N > 1$, there exists no aperture, $f(x,y)$, that satisfies (1) the N constraints corresponding to the pupils, (2) the Helmholtz equation and (3) the constant area constraint of in Equation 6. The convex sets corresponding to these constraints thus have a null intersection. The convex constraint corresponding to a specific plane and the set corresponding to Equation 6, however, have a nonempty intersection. POCS therefore converges for the case of a single image.

In order to improve the image quality, the pupil constraint sets on the N planes will be fuzzified.[4] In lieu of requiring the function to be zero outside of the pupil, an allowance is made for leakage. As in Equation 4, $q_n(x,y) = g_n(x,y)$ inside the pupil. Outside of the pupil,

$$q_n(x,y) = \begin{cases} g_n(x,y) & ; \ ||g_n(x,y)|| \le t_n(\alpha) \\ \frac{t_n(\alpha)}{||g_n(x,y)||}g_n(x,y) & ; \ ||g_n(x,y)|| > t_n(\alpha) \end{cases} \quad (7)$$

where $t_n(\alpha)$ is a threshold that is a decreasing function of α and

$$||g(x,y)||^2 = \int_{-\infty}^{\infty}\int_{-\infty}^{\infty} |g(x,y)|^2\,dx\,dy$$

Examples

In the two examples to follow, $N = 3$, $z_1 = 200{,}000\ \lambda$, $z_2 = 400{,}000\ \lambda$, and $z_3 = 600{,}000\ \lambda$. Also, because it gave good results, we used

$$t_n(\alpha) = -(n-0.9)^2 \ln(\alpha)\ ;\ n = 1,2,3. \quad (8)$$

This function is increasing with n for reasons that will soon become apparent.

[3] A linear variety.

[4] Since it is specified by physics rather than desired synthesis constraints, the Helmhotz equation must, of course, be left crisp.

Propagating Faces

In this example, in order to their closeness to the aperture, the pupils correspond to the outlines of a frowning face, an emotionless face and a happy face. The results for conventional POCS is shown in Figure 8 are in the bottom row. The noise level in the POCS solution increases with the distance from the aperture. Therefore, one can be more lenient with the α-cut level close to the aperture than one farther away. For this reason, the function in Equation 8 increases with respect to n. The conventional POCS solution in Equation 8 corresponds to $\alpha = 1$. As the α cut is increased, there is more of a sharing of the diffuse background noise among the three images. Eventually, the noise shifts to the image closest to the aperture.

Three Line Images

The propagating faces example was repeated for three line drawings - a plane, a dinosaur and a tiger. The results are shown in Figure 9 for two α cuts. Shown are two sets of four pictures. In each set, the aperture in the upper left is the magnitude of the transmittance. The fuzzy POCS tuning in the bottom set of four images results in the perception of the airplane whereas the top set of four images does not.

III. Tomographic Image Synthesis

The fundamental problem in tomography is reconstruction of an object from its projections[5]. Illustration will be made for the case of tomographic reconstruction using limited angle parallel beam data [23]. Conventional POCS has been applied to tomographic reconstruction with some quite remarkable results [26].

Let $f(x,y)$ denote a two dimensional object to be reconstructed, such as the Shepp-Logan phantom [24] in Figure 10, and $F(u,v)$ its Fourier transform.

$$F(u,v) = \int\int_{\text{aperture}} f(x,y)e^{-j2\pi(ux+vy)}dxdy$$

The transform of $f(x,y)$ is known only in the shaded region pictured in Figure 11. Although any limited angle can result in practice, after Jaffe [23], we assume an angle of the wedge in Figure 11 is 90^0. Let

$$A(u,v) = \begin{cases} 1 & ;\text{inside the shaded region} \\ 0 & ;\text{outside} \end{cases}$$

The observed (or *naive* [23]) object is given by the inverse Fourier transform

$$f_{obs}(x,y) = \int_{-\infty}^{\infty}\int_{-\infty}^{\infty} A(u,v)F(u,v)e^{j2\pi(ux+vy)}dudv$$

[5] The term 'projection' here differs in meaning from a projection used in POCS. The distinction will be made clear in the context of its use.

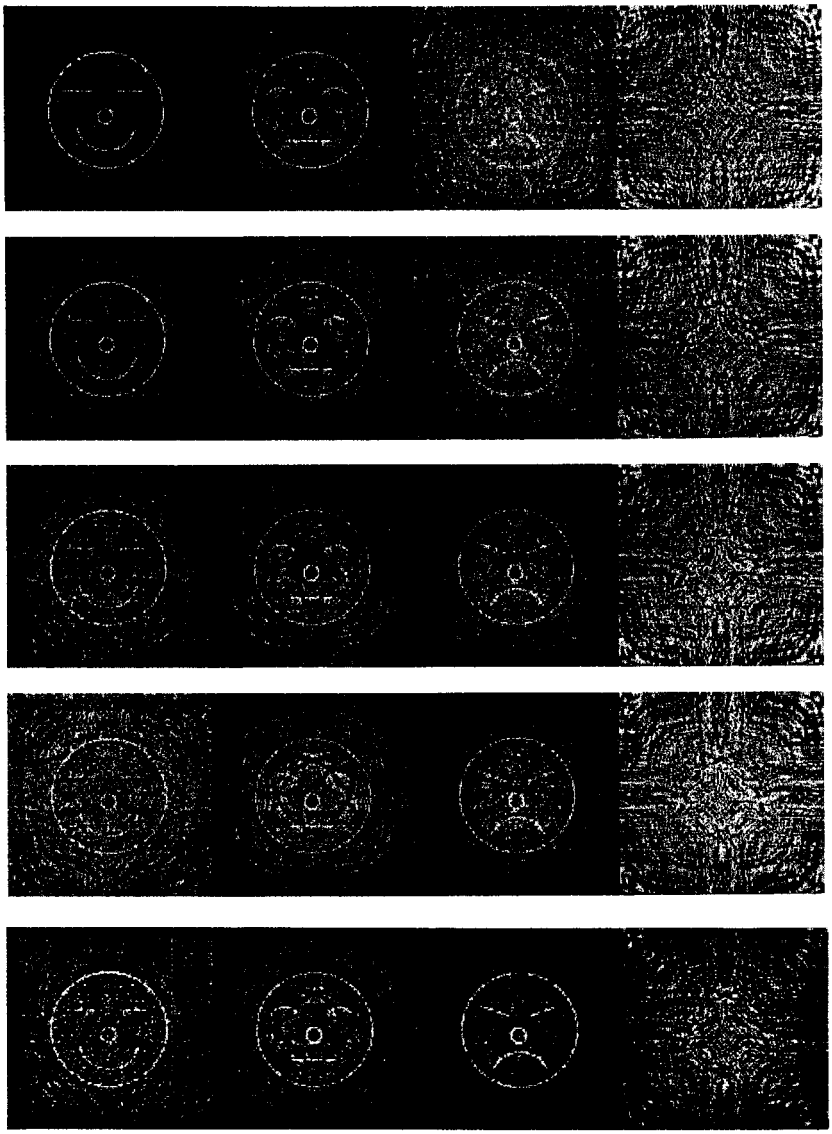

Figure 8: Propagating Faces: The right column is the magnitude of the diffracting aperture synthesized using fuzzy POCS. From left to right, the resulting diffraction is shown for $z_3 = 600.000\ \lambda$, $z_2 = 400.000\ \lambda$, and $z_1 = 100.000\ \lambda$. For $a^2 = -300\ \ln(\alpha)$, the α cuts correspond to $a = 0.0$ for the bottom row (conventional POCS), $a = 0.02$, $a = 0.03$, $a = 0.04$, and $a = 0.05$ (top row). As a increases, α decreases, and more emphasis is given to the sharpness (lack of diffuse background noise) of the image farthest from the aperture.

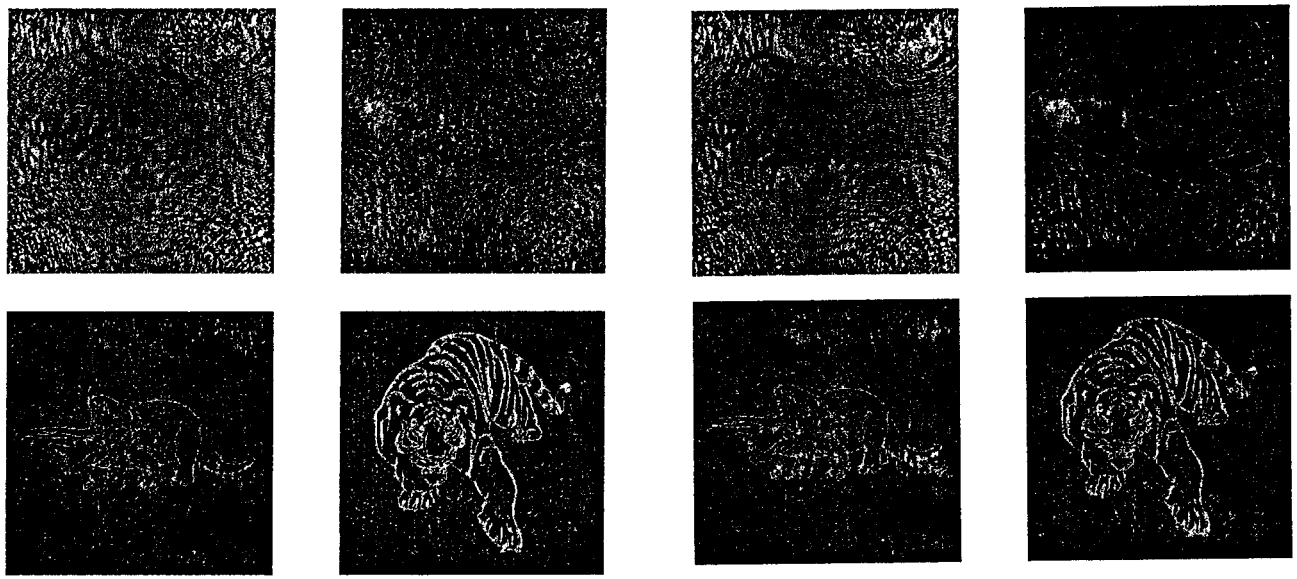

Figure 9: Three line drawings (airplane, dinosur and tiger) are used for the pupil functions in the three planes. The parameters are identical to those in the previous figure. For the right hand set of four figures, $a = 0.03$ whereas $a = 0.02$ for the left hand set of four. The airplane is visible for $a = 0.02$ and lost in diffuse background noise for $a = 0.03$.

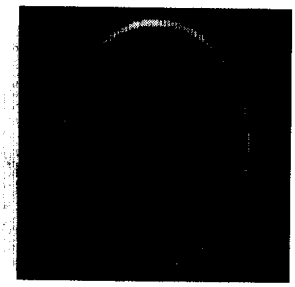

Figure 10: The Shepp-Logan phantom.

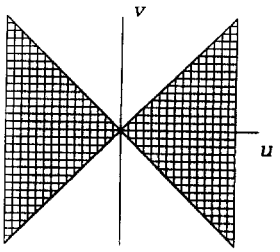

Figure 11: The transform of the image to be restored is known only within the shaded region.

The restoration problem is to find $f(x,y)$ from $f_{obs}(x,y)$. The unconstrained problem is ill-posed [25].

Peng and Stark [32] imposed the following convex constraints on the reconstruction problem.

1. **Spectral constraint** The desired object, $f(x,y)$, is known to have a transform that is equal to the Fourier transform of $f_{obs}(x,y)$ in the shaded region in Figure 11. The set of all objects satisfying this constraint form a convex set[6] The naive image corresponding to the phantom in Figure 10 is shown in Figure 13.

2. **Image support**. The desired object is known to be zero outside of the region of support. The set of all objects satisfying this constraint forms a convex set[7]. To project an arbitrary object onto this set, the function is set to zero outside of the region of support which, in the case of the phantom in Figure 10, is the large oval.

3. **Bounded.** The restored object must lie in the interval
$$0 \leq f(x,y) \leq b$$
where b is a chosen upper bound. The set of signals satisfying this constraint form a convex set[8]. To project onto this set, all values below zero are set to zero and all values above b are set to b. For the example to follow, $b = 1$.

4. **Energy constraint**. The energy of a function, $g(x,y)$, is defined as $E = ||g(x,y)||^2$. The set of all signals with energy not exceeding a specified energy form a convex set[9]. To project onto this set, a signal $g(x,y)$ is multiplied by
$$\frac{\sqrt{E}}{||g(x,y)||}$$
if the energy of g exceeds the specified energy. The signal is left unaltered otherwise.

5. **Reference constraint.** A reference object, say $f_r(x,y)$, is known from a previous reconstruction of from heuristics. For the example to follow, the reference shown in Figure 12 is used. Compared to the phantom in Figure 10, note that the small details have been removed and the sizes of the ovals reduced by 20% of their linear dimension. The restored function is assumed not to deviate significantly from this reference. The set of functions $\{f(x,y)\}$ for which
$$||f(x,y) - f_r(x,y)|| \leq r$$
form a convex set[10]. If an object, $g(x,y)$ does not obey this constraint, it can be projected onto the set by merely subtracting $f_r(x,y)$ and multiplying by
$$\frac{r}{||g(x,y) - f_r(x,y)||}$$

Starting with an object that is zero, projection onto each of these convex sets was repeated until convergence.

Crisp POCS was applied to the restoration using $r =$ 10% of $||f(x,y)||$ and $E = 1998$. The result, shown in Figure 14, shows significant reconstruction artifacts. In Figure 15, the structure internal to the reference phantom has been dilated using a circular dilation kernel and the energy increased to $E = 2472$. These parameters result in a more accurate estimation of the dimensions of the original phantom. Application of POCS to this fuzzification results in fewer artifacts and a stronger appearance of the finer structure in the target phantom.

[6] A linear variety.
[7] A subspace
[8] A cube if b is not a function of (x,y). Otherwise, a box.
[9] A ball.
[10] A ball of radius r centered at $f_r(x,y)$.

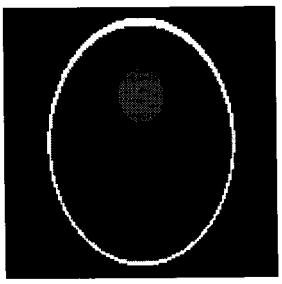

Figure 12: The reference image used in POCS.

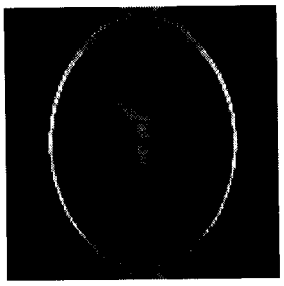

Figure 13: The naive image of the phantom.

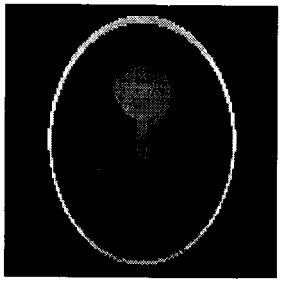

Figure 14: The restoration using conventional POCS.

Figure 15: The restoration using fuzzy POCS.

References

[1] H. Stark, editor, **Image Recovery: Theory and Application**, (Academic Press, Orlando, 1987).

[2] D.C. Youla and H. Webb, "Image restoration by method of convex set projections: Part I - Theory", *IEEE Trans. Med. Imaging*, vol MI-1, pp.81-94, 1982.

[3] M.H. Goldburg and R.J. Marks II "Signal synthesis in the presence of an inconsistent set of constraints", *IEEE Transactions on Circuits and Systems*, vol. CAS-32 pp. 647-663 (1985).

[4] J. Von Neumann, **Continuous Geometry**, Edwards Brothers, Ann Arbor, Michigan, 1937.

[5] L. M. Bregman, "Finding the common point of convex sets by the method of successive projections", *Doki. Akad. Nauk. USSR*, vol 162, no. 3, pp.487-490, 1965.

[6] L. G. Gubin, B. T. Polyak and E. V. Raik, "The method of projections for finding the common point if convex sets", *USSR Comput. Math. Phys.*, vol 7, no. 6, pp.1-24, 1967.

[7] J. Von Neumann, **The Geometry of Orthogonal Spaces**, Princeton University Press, Princeton, New Jersey, 1950.

[8] Hidegorô Nakano, **Spectral Theory in the Hilbert Space**, Japan Society for the Promotion of Science, Ueno Park, Japan, 1953.

[9] M.I. Sezan and H. Stark, "Image restoration by method of convex set projections: Part II - Applications and Numerical Results", *IEEE Trans. Med. Imaging*, vol MI-1, pp.95-101, 1982.

[10] D.C. Youla and V. Velasco, "Extensions of a result on the synthesis of signals in the presence of inconsistent constraints", *IEEE Transactions on Circuits and Systems*, vol. CAS-33, pp.465-468 (1986).

[11] Didier Dubois and Henri Prade, **Fuzzy Sets and Systems: Theory and Applications**, Academic Press, Boston, 1980.

[12] L. Zadeh, "Fuzzy Sets", **Information Control**, vol.8, pp.338-353, 1965. Reprinted in J.C. Bezdek & S.K. Pal, **Fuzzy Models for Pattern Recognition**, (IEEE Press, 1992).

[13] L.T. Koczy and K. Hirota, "Ordering, distance and closeness of fuzzy sets", **Fuzzy Sets and Systems**, vol.59, no.3. pp. 281-93. Nov. 10, 1993.

[14] M.R. Civanlar and H.J. Trussel, "Digital signal restoration using fuzzy sets", *IEEE Transactions on Acoustics, Speech and Signal Processing*, vol. ASSP-34, p.919 (1986).

[15] Feiyue Zhou, "The relative interiors of convex fuzzy sets under induced fuzzy topology", **Fuzzy Sets and Systems**, vol.44, no.1. pp. 109-125. Nov. 5, 1991.

[16] Feiyue Zhou, " The recession cones and Caratheodory's theorem of convex fuzzy sets", **Fuzzy Sets and Systems**, vol.44, no.1. pp. 57-69, Nov. 5, 1991.

[17] S. Oh and R.J. Marks II, "Alternating projections onto fuzzy convex sets", *Proceedings of the Second IEEE International Conference on Fuzzy Systems* (FUZZ-IEEE '93), San Francisco, March 1993, vol.1, pp. 148-155.

[18] J.C. Bezdek, **Pattern Recognition with Fuzzy Objective Function Algorithms**, Plenum Press, New York, 1981.

[19] J. Serra, **Image analysis and mathematical morphology**, (Academic Press, New York, 1982).

[20] P. Maragos and R. W. Schafer, "Morphological filters - Part I: Their set-theoretic analysis and relations to linear shift-invariant filters", *IEEE Trans. on Acoustic, Speech, and Signal Processing*, vol.ASSP-35, no.8 , 1987. pp.1153-1169.

[21] F.P. Preparata and M.I. Shamos, **Computational Geometry: An Introduction**, Springer-Verlag, New York, 1985, p.172.

[22] P.M. Hirsch, J.A. Jordon, Jr., and L.B. Lesem, "Method of making an object-dependent diffuser," U.S. Patent No. 3,619,022 (November 9, 1971).

[23] J.S. Jaffe, "Limited angle reconstruction using stabalized algorithms", *IEEE Transactions on Medical Imaging*, vol.9, pp.338-343 (1990).

[24] T. Olson and J.S. Jaffee, "An explanantion of the effects of squashing in limited angle tomography", *IEEE Transactions on Medical Imaging*, vol.9, no.3, (1990).

[25] R.J. Marks II, "Posedness of a bandlimited image extension problem in tomography", *Optics Letters*, vol.7, pp.376-377 (1982).

[26] M.I. Sezan and H. Stark, "Tomographic image reconstruction from incomplete view data by convex projections and direct Fourier inversion," *IEEE Transactions on Medical Imaging*, vol.MI-3, pp. 91-98, June, 1984.

[27] J.A. Reeds and L.A. Shepp, "Limited angle reconstruction in tomography via squashing", *IEEE Transactions on Medical Imaging*, vol.MI-6, pp.89-97, June 1987.

[28] J. Goodman, **Introduction to Fourier Optics**, McGraw Hill, New York, 1968.

[29] P. Maragos and R. W. Schafer, "Morphological filter - Part I: Their set-theoretic analysis and relations to linear shift-invariant filters", *IEEE Trans. on Acoustic, Speech, and Signal Processing*, vol.ASSP-35, no.8, 1987. pp.1153-1169.

[30] R.M. Mersereau and A.V. Oppenheim, "Digital reconstruction of multidimensional signals from their projections", *Proceedings of the IEEE*, vol.62, no.10, pp.1319-1338, 1974.

[31] A.C. Kak and M.Slaney, Editors, **Principles of Computerized Tomographic Imaging**, IEEE Press, 1987.

[32] H.Peng and H.Stark, "Direct Fourier Reconstruction in Fan-Beam Tomography", *IEEE Transactions on Medical Imaging*, vol.MI-6, pp.209-219, September 1988.

[33] A. Papoulis, "A new algorithm in spectral analysis and bandlimited signal extrapolation", *IEEE Transactions on Circuits and Systems*, vol.CAS-22, pp.735-742 (1975).

[34] R.J. Marks II, **An Introduction to Shannon Sampling and Interpolation Theory**, (Springer-Verlag, 1991).

[35] S. Kuo and R.J. Mammon, "Resolution enhancement of tomographic images using the row action projection method", *IEEE Transactions on Medical Imaging*, vol.10, no, pp.593-601 (1992).